

PAPER • OPEN ACCESS

## Methodology of constructing highly adequate models of additively manufactured materials

To cite this article: A I Borovkov *et al* 2020 *IOP Conf. Ser.: Mater. Sci. Eng.* **986** 012034

View the [article online](#) for updates and enhancements.

### You may also like

- [Laser shock peening and its effects on microstructure and properties of additively manufactured metal alloys: a review](#)  
Michael Munther, Tyler Martin, Ali Tajyar *et al.*
- [Coupling between feedback loops in autoregulatory networks affects bistability range, open-loop gain and switching times](#)  
Abhinav Tiwari and Oleg A Igoshin
- [Fatigue life prediction of the additively manufactured specimen](#)  
Surajit Kumar Paul, Faris Tarlochan and Timothy Hilditch

### Recent citations

- [Approaches to testing vehicle passive safety based on a virtual test bench and a digital twin](#)  
Dmitry Bogdanov *et al*
- [Development of elastic-plastic model of additively produced titanium for personalised endoprosthetics](#)  
Alexey Borovkov *et al*
- [Load distribution method in helicopter blade multibody dynamics system](#)  
Anton Didenko *et al*



The Electrochemical Society  
Advancing solid state & electrochemical science & technology

## 241st ECS Meeting

May 29 – June 2, 2022 Vancouver • BC • Canada

Extended abstract submission deadline: Dec 17, 2021

Connect. Engage. Champion. Empower. Accelerate.  
**Move science forward**



**Submit your abstract**



# Methodology of constructing highly adequate models of additively manufactured materials

A I Borovkov<sup>1</sup>, L B Maslov<sup>1,2</sup>, K S Ivanov<sup>1</sup>, E N Kovaleva<sup>1</sup>, F D Tarasenko<sup>1</sup>, M A Zhmaylo<sup>1</sup> and Barriere Thierry<sup>3</sup>

<sup>1</sup>Center of National Technological Initiative, Institute for Advanced Manufacturing Technologies, Peter the Great St. Petersburg Polytechnic University, 29 Politekhnicheskaya, St. Petersburg, 195251, Russia, E-mail address: tarasenko@compmechlab.ru

<sup>2</sup>Department of Theoretical and Applied Mechanics, Ivanovo State Power Engineering University, 34 Rabfakovskaya, Ivanovo, 153003, Russia

<sup>3</sup>Applied Mechanics Department, Institute “Franche-Comté Electronics Mechanics Thermal Science and Optics – Sciences and Technologies”, 15B avenue des Montboucons, Besançon, France 25030

**Abstract.** In the this paper there is a description of the methodology of constructing highly adequate models of materials which are produced additively. The paper consists of introduction to the problem, demonstration of each step of the methodology and conclusions about the method and its applicability. The developed approach is presented on the two additively manufactured metal alloys. The modeling process is based on the orthotropic model of elasto-plastic material behavior. The list of material properties to be found was formulated according to proposed material model. These properties were found from several mechanical experiments. The developed mathematical models of the material studied were checked for compliance to experimental data with use of finite element simulations. Finite element modeling of a complicated 3d-printed lattice structure was performed and compared with the results of natural testing. In order to study the correlation between the material properties and manufacturing process the analysis of microstructure was done.

## 1. Introduction

This paper represents the methodology of material modeling for parts which are manufactured from metal powders with 3d-printing approaches. This methodology suggests a clear and easy way to construct such material models for further usage in finite elements simulations.

Additive manufacturing is one of the most rapidly developing advanced manufacturing technology [1]. The use of this technology removes a large number of traditional manufacturing barriers and obstacles [2]. That's why now it becomes possible to develop parts which producing was economically unreasonable or unfeasibly at all. Such manufacturing capabilities lead to significant changes in design approach. Now the goal of a part design is to implement the potential of additive manufacturing as efficiently as possible in order to get competitive products. This competitive product should consist of optimal decisions in each and every step of its lifecycle, from development to manufacturing.

One of these steps is quality of a material model. Utilized material model should match the high level of developing and manufacturing complicity and accuracy, and should be as close to reality as possible. That's why the main aim of this study is to develop a methodology for constructing highly adequate



mathematical models of continuous materials, which are produced from metal powder with layer-by-layer technology, e.g. selective laser melting (SLM) or electron beam melting (EBM) [3, 4].

Performed analysis of papers about the same topic [5, 6, 7] showed that the comprehensive testing and analysis of additively produced materials is a live issue. But it is necessary to mention that in most cases only simple material models (like elastic isotropic ones) were used. Only few papers propose a hypothesis that the printed materials must be considered from the continuum mechanics point of view with using the anisotropic mathematical models [8, 9]. This all confirms the relevance of performed study.

So, the main aim of this study is the process of constructing material models based on the elastic and plastic anisotropic continuum media, which will match real life material behavior better than widely used elastic isotropic ones.

Onwards the developed methodology is performed for two well-known and widely used metallic materials, aluminum alloy AlSi10Mg and titanium alloy Ti6Al4V, and samples additively produced by using SLM machine for the aluminum alloy and EBM machine for the titanium alloy.

## 2. Methodology concept

First of all, the choice of material model type should be done. Chosen type of material model should be strongly connected with the purposes of model construction. For example, the model of materials used in thermonuclear reactors must include mechanical, thermodynamic and electromagnetic equations to describe all the possible processes. Talking about a way of usage additively manufactured parts, then their most common application are structures or construction parts. Thus, the mechanical behavior of the material is the main point of interest in this study.

Next step in the defining of a material model type is taking into account the influence of the manufacturing process on the material behavior. Here and later in this study, we are based on the assumption that additive manufacturing process strongly affects mechanical properties of a material.

The research of microstructure of considered materials was performed to figure out the type of its' behavior. On the below figures (1,2) obtained by using electronic microscopy we can observe the microstructure of AlSi10Mg and Ti6Al4V specimens.

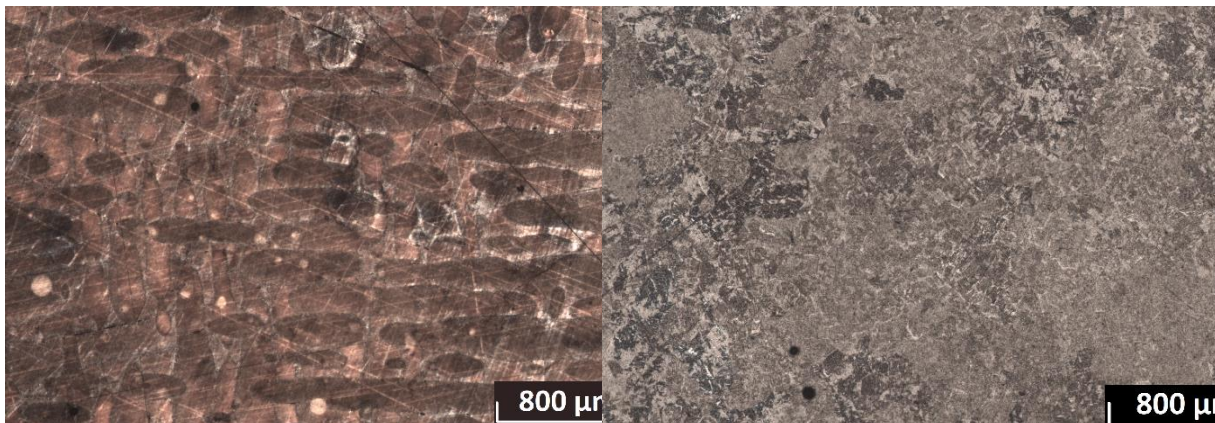


**Figure 1.** Microstructure of AlSi10Mg specimen.

**Figure 2.** Microstructure of Ti6Al4V specimen.

On the pictures above there is a demonstration of microstructure in a cross-section of specimens made normal to the printing direction. Main conclusion that can be made here in terms of material behavior is that these structures might provide anisotropic properties of the material on macroscale. It is clearly visible on the Figure 1 where crystallites have pronounced elongation in two directions.

The microstructure on the above pictures is observed in a cross-section of each specimen made normal to the printing direction. On the Figure 1 it is clearly visible that crystallites have pronounced elongation in two directions. This fact leads to a conclusion that these structures might provide anisotropic properties of the material behavior on macroscale.

Characteristics of considered additive manufacturing processes and the conclusion made above allows to focus the methodology on the orthotropic model of elasto-plastic behavior.

Generally, the methodology proposed consists of several steps as follows:

- mathematical formulation of the material model based on the continuum mechanics approaches;
- identification of the equation material constants from the experiment;
- model verification.
- In this paper an additional step with the demonstration of applying constructed material model is performed.

### 3. Mathematical model of the material

#### Elasticity

In this study the orthotropic elasto-plastic model is constructed step-by-step. First of all, the elastic behavior is formulated by Hooke's law in tensor notation [10],

$$\boldsymbol{\sigma} = \mathbf{C} \cdot \boldsymbol{\varepsilon} \quad (1)$$

where  $\boldsymbol{\sigma}$  – Cauchy stress tensor;  $\mathbf{C}$  - elasticity tensor;  $\boldsymbol{\varepsilon}$  – strain tensor.

The formula 1 can be represented in the inverse form in matrices notations and with use of the engineering constants:

$$\begin{Bmatrix} \varepsilon_{xx} \\ \varepsilon_{yy} \\ \varepsilon_{zz} \\ \gamma_{xy} \\ \gamma_{xz} \\ \gamma_{yz} \end{Bmatrix} = [S] \cdot \begin{Bmatrix} \sigma_{xx} \\ \sigma_{yy} \\ \sigma_{zz} \\ \sigma_{xy} \\ \sigma_{xz} \\ \sigma_{yz} \end{Bmatrix} \quad (2)$$

where  $[S]$  – compliance tensor in matrix form:

$$[S] = \begin{pmatrix} \frac{1}{E_x} & -\frac{\mu_{xy}}{E_x} & -\frac{\mu_{xz}}{E_x} & & & \\ -\frac{\mu_{yx}}{E_y} & \frac{1}{E_y} & -\frac{\mu_{yz}}{E_y} & & & \\ -\frac{\mu_{zx}}{E_z} & -\frac{\mu_{zy}}{E_z} & \frac{1}{E_z} & & & \\ & & & \frac{1}{G_{xy}} & 0 & 0 \\ & 0 & & 0 & \frac{1}{G_{xz}} & 0 \\ & & & 0 & 0 & \frac{1}{G_{yz}} \end{pmatrix} \quad (3)$$

The following notation was used in the formula above:

$E_i$  – Young's modulus

$G_{ij}$  – shear modulus

$\mu_{ij}$  – Poisson's ratio

We can observe twelve different material constants in the equation 3. However, there are three additional equation defining the relation between these constants. So, only nine of them are independent. Therefore, in order to fully describe elastic behavior of the material it is necessary to find these nine constants: three Young's moduli, three shear moduli, three Poisson's ratios

#### Plasticity

After defining the elastic behavior, the yield criterion should be formulated. The assumption of the orthotropy in material properties makes it impossible to utilize von Mises yield criterion as it can't describe differences in values of yield stress in proposed directions. Hill yield criterion is one of the most common way to describe the moment of transition to plasticity in case of orthotropic material. It can be represented in several ways. In this study the following equation was used [11]:

$$\sigma_{eq} = \sqrt{\frac{3}{2(H + F + G)} (H(\sigma_{xx} - \sigma_{yy})^2 + F(\sigma_{yy} - \sigma_{zz})^2 + G(\sigma_{zz} - \sigma_{xx})^2 + 2N\sigma_{xy}^2 + 2M\sigma_{xz}^2 + 2L\sigma_{yz}^2)}$$

$$\sigma_{eq} \geq \sigma_y \quad (4)$$

where  $\sigma_{eq}$  – equivalent stress; H, F, G, N, M, L – coefficients of material;  $\sigma_y$  – threshold (yield) stress. Six material constants H, F, G, N, M, L in the criterion (4) can be calculated from the values of yield stresses in each direction including shear ones. These six constants in the criterion allow to define the transition to plasticity by one specific value of threshold stress which will be compared to equivalent one calculated by the formula (4). According to this fact it is necessary to obtain six values of yield stress to define the yield criterion. These six values are three tension yield stresses and three shear yield stresses.

The last step in the process of defining the orthotropic elasto-plastic material model is description of the plastic material behavior. One of the possible ways here is to use stress-strain curve constructed from several specific points. Axes of this curve should be assigned as follows: abscissa is equivalent stress, calculated by the formula (4), and ordinate presents plastic strain. This choice should provide an alignment of stress-strain curves of any type and direction of loading. This means that chosen axes “scale” these curves and fit them to the one.

#### 4. Testing and experimental data processing

##### Testing description

The list of material properties to obtain is formulated according to proposed material model. These properties are supposed to be found from several mechanical experiments: uniaxial tension in three directions and uniaxial torsion around three axes.

Tension experiments provide information about Young’s moduli, Poisson’s ratios and three yield curves. Specimens with circle cross-section for tension experiments are designed according to [12] and presented on Fig. 3.

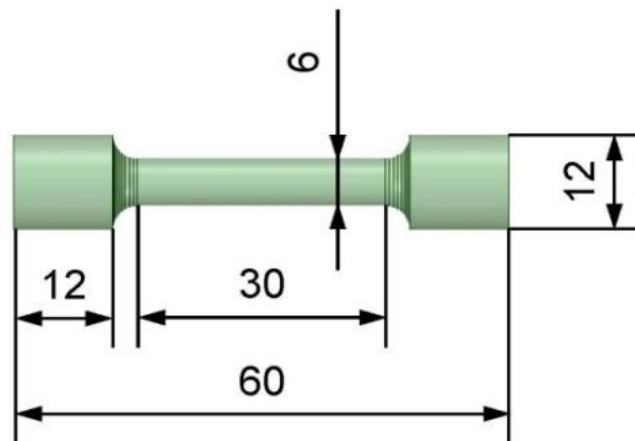


**Figure 3.** Uniaxial tension specimen (sizes provided in mm).

To carry out tension tests a test machine Zwick Z250 was used. Also the laser extensometer Zwick LaserXtens HP was used in order to measure transverse strain for Poisson’s ratio estimation.

The torsion experiments give information about shear moduli and another three yield curves. Specimens with circle cross-section for torsion experiments are designed according to [13] and presented on Fig. 4.

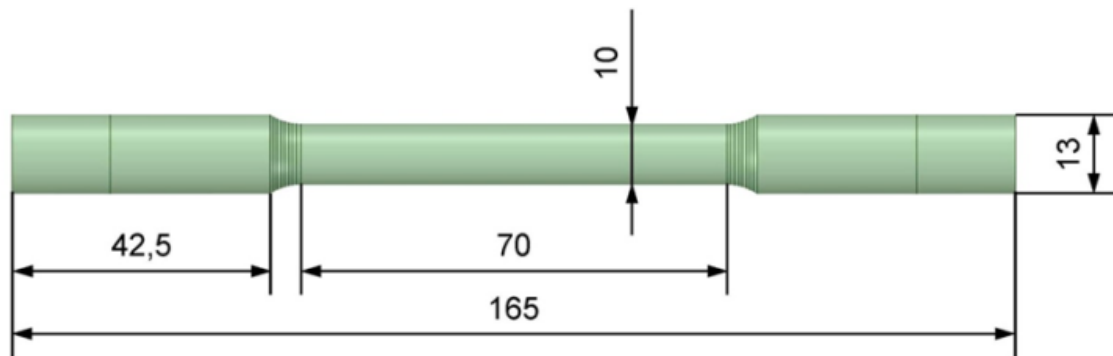


**Figure 4.** Uniaxial torsion specimen (sizes provided in mm).

A test machine Instron 8850 was used to carry out torsion tests.

Because of the assumption about orthotropic material behavior it is required to test each type of described loading in three directions. These directions should match the principal axes of anisotropy of a material. That's why it was decided to align the direction of loading of each specimen with the axes of the printing machine. The figure 5 is demonstrating the torsion specimens' orientation during printing process. Orientation of tension specimens was made in the same way.

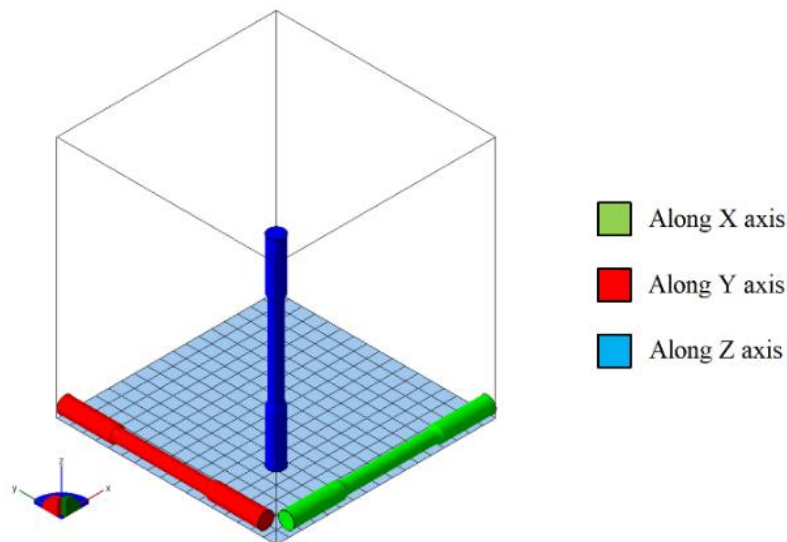


**Figure 5.** Torsion specimens' orientation.

To obtain values of desired material properties it is necessary to process the experimental data. The results of performed tests to process are stress-stain (load-displacement) curves.

In terms of minimizing the influence of random factors like manufacturing defects a set of three specimens for each orientation and type of loading is produced. Such specimens' amount makes it possible to perform a statistical processing of required values.

#### 4.1. Experimental data processing

The processing of each coefficient of the model is based on techniques described in [12, 13, 14].

Young's modulus and tension yield stress of one direction obtaining is performed iteratively as follows. On a stress-strain curve a linear section is selected. Bounds of this section are determined based on the expected value of yield stress. Lower bound is 10% of this value, upper is 85%. This is needed to exclude all nonlinearities. Using the least squares method, a linear approximation of this section is done. A coefficient of this approximation is an applicant for the Young's modulus value. Afterwards plastic strain values are calculated by the subtraction of elastic strain from full ones. The stress value which

corresponds to 0.2% plastic strain value is considered to be the yield stress value. If this value is equal to the expected yield stress value used in the beginning of the process, we consider that processing is completed and values are final. If not, we repeat the process with use the obtained yield stress value as new expected one. The described process is visually presented as a diagram on the Figure 6.

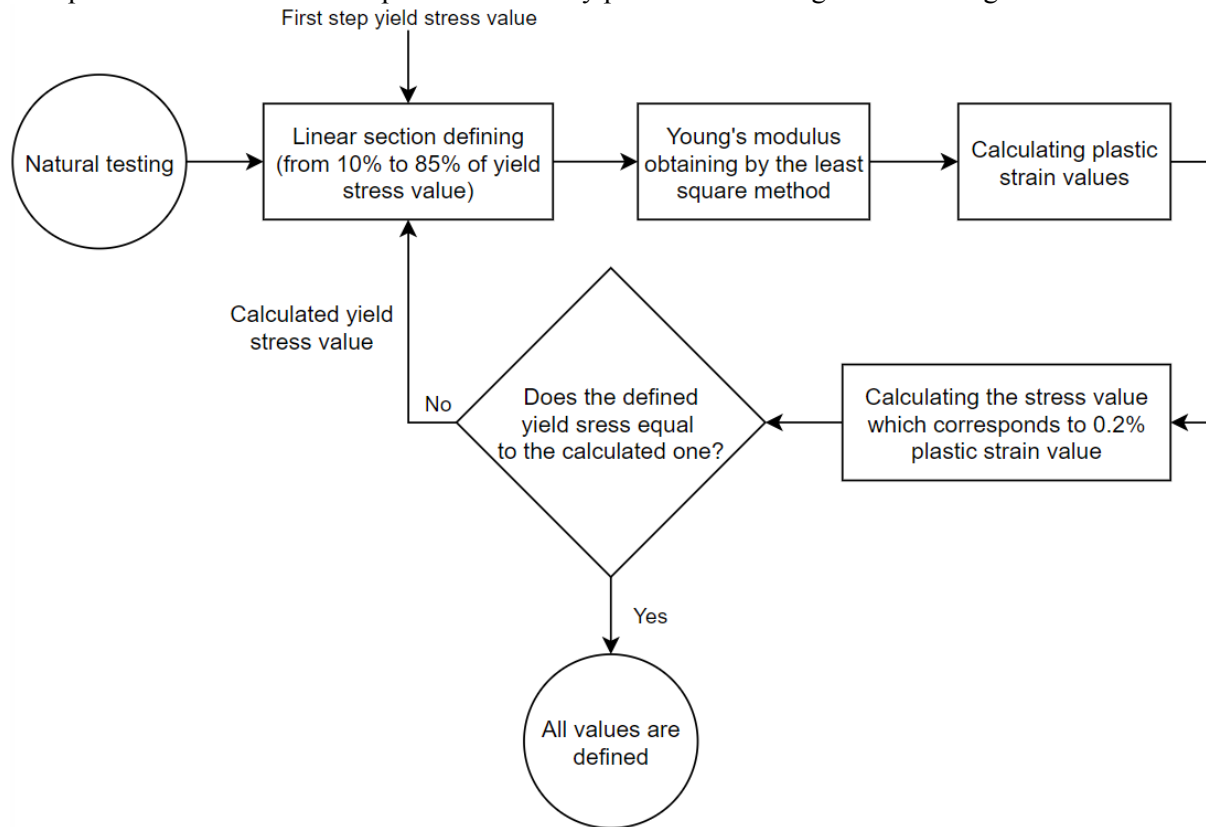


**Figure 6.** Tension test data processing diagram.

The process described above is performed for each tested specimen. So, each required value (Young's modulus and tension yield stress) is defined three times. This allows to calculate the final value as average from three available ones.

To estimate the value of the Poisson's ratio it is required to use results of measuring transverse strain values. The value of Poisson's ratio is calculated as a relation between the transverse strain to the axial strain measured in the linear section of stress-strain curve. As well as in the case of Young's modulus the final value of the Poisson's ratios in each direction is calculated as an average from three available ones.

All described processing techniques are relatively widely used and there is no effect on them from the proposed material model type. But in case of torsion problem it is impossible to easily use these methods, due to assumption about orthotropic material behavior. As it was mentioned before, obtaining the values of shear moduli is based on results of uniaxial torsion experiments. Its procedure is clear and easy in case of isotropic material model [13]. The value of shear modulus is calculated just as a ratio of shear stress to shear strain in a linear part of stress-strain curve. But if we take into account the assumption about orthotropic behavior the stress-strain state will be noticeably different. That's why in case of torsion problem it is necessary to perform an additional research.

Calculation submitted below are based on the anisotropic models of continuum mechanics [10].

First of all, we consider that we get the amount of values of torque and twist angle as a result of torsion tests. We assume the uniaxial torsion is performed about Z axis (Fig. 7).

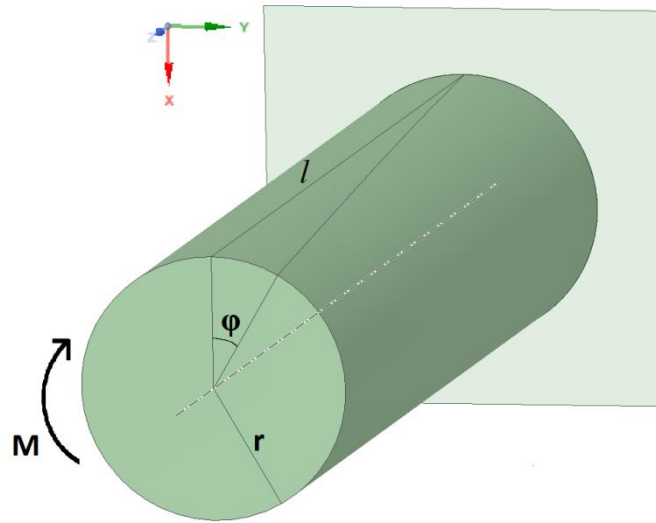


**Figure 7.** The statement of a torsion problem.

Let's assume the following relation between torque and twist angle:

$$\varphi = \frac{M}{C} \quad (5)$$

Second thing to mention is that there are two independent shear moduli which affect the stress-strain state during the uniaxial torsion along proposed axis. In case of torsion about Z axis these two moduli are  $G_{xz}$  and  $G_{yz}$ . This means that the relation between torque and twist angle includes both these moduli. We can describe the relation between torque and twist angle as torsional stiffness which can be calculated for circled cross-section as follows [10]

$$C = \frac{\pi r^4}{\left(\frac{1}{G_{xz}} + \frac{1}{G_{yz}}\right)} \quad (6)$$

From the above equation it is clear that it is impossible to get the values of two independent shear moduli from the results on one test. To resolve this problem all below calculations are performed.

We can obtain the following equation based on previous two

$$\varphi = \frac{M}{2J_p} \left( \frac{1}{G_{xz}} + \frac{1}{G_{yz}} \right) \quad (7)$$

And finally let's introduce B as follows

$$\frac{1}{B_z} = \frac{1}{2} \left( \frac{1}{G_{xz}} + \frac{1}{G_{yz}} \right) \quad (8)$$

Now the value of twist angle can be calculated in this way

$$\varphi = \frac{M}{J_p B_z} \quad (9)$$

These steps allow us to have the value which is possible to obtain from one experiment. This value is introduced to represent an average response of the material to the torsion loading in terms of two shear moduli. Main idea here is that it becomes possible to find the value of B with the procedure from [13] which relatively copies the procedure of obtaining Young's moduli. Now to get the value of each shear moduli we need obtaining same two values of B from experiments along X and Y axes. After this step we have three B values which are defined as follows



$$\begin{cases} \frac{2}{B_z} = \left( \frac{1}{G_{xz}} + \frac{1}{G_{yz}} \right) \\ \frac{2}{B_y} = \left( \frac{1}{G_{xy}} + \frac{1}{G_{yz}} \right) \\ \frac{2}{B_x} = \left( \frac{1}{G_{xz}} + \frac{1}{G_{xy}} \right) \end{cases} \quad (10)$$

This nonlinear system of equations has the following solution

$$\begin{cases} G_{xy} = \frac{B_x B_y B_z}{(-B_x B_y + B_x B_z + B_y B_z)} \\ G_{xz} = \frac{B_x B_y B_z}{(B_x B_y - B_x B_z + B_y B_z)} \\ G_{yz} = \frac{B_x B_y B_z}{(B_x B_y + B_x B_z - B_y B_z)} \end{cases} \quad (11)$$

Now all the required values of shear moduli are obtained.

Torsion yield stresses obtaining is also connected with the same difficulties caused by the problem explained above. All these difficulties can be resolved with calculations based on [10] and [11]. These analytical calculations are performed with a relatively same approach. The idea of these calculations is to obtain a full stress-strain state of a specimen up to the moment of transition to plasticity. Plastic strain values can be calculated with use of already processed shear moduli. The stress value at the moment when plastic strain reaches 0.2% is taken as shear yield stress.

#### 4.2. Material properties obtained

Following Tables 1-3 contain several results of experimental data processing in all proposed directions.

**Table 1.** AlSi10Mg material properties.

Material property/ Direction	X/XY	Y/YZ	Z/XZ
Young's modulus [GPa]	82.5	76.7	76.8
Shear modulus [GPa]	23.8	27.1	21.4
Tension yield stress [MPa]	227.8	232.8	217.7
Torsion yield stress [MPa]	132.9	135.7	140.4
Poisson's ratio	0.32	0.32	0.33

**Table 2.** Ti6Al4V material properties.

Material property/ Direction	X/XY	Y/YZ	Z/XZ
Young's modulus [GPa]	124.2	121.9	124.1
Shear modulus [GPa]	37.5	41.8	42.0
Tension yield stress [MPa]	983.7	980.9	964.2
Torsion yield stress [MPa]	588.6	525.8	571.1
Poisson's ratio	0.26	0.25	0.26

**Table 3.** Parameters of Hill's plasticity models for AlSi10Mg and Ti6Al4V.

Parameter type	F	G	H	L	M	N
AlSi10Mg	0.517	0.559	0.424	1.444	1.293	1.384
Ti6Al4V	0.515	0.510	0.479	1.724	1.461	1.375

Values summarized in Tables 1-3 show that the materials studied have properties variations in different directions. This means that the assumption about anisotropic behavior was done correctly and that chosen model describes material closer to the real life than widely used elastic isotropic one.

These constants will be used in further finite element simulation and analysis of the obtained results.

## 5. Model verification

### Models description

Two constructed material models were checked for compliance to experimental data. Calculations were performed in SIMULIA Abaqus for each test's direction. An orthotropic elasto-plastic material model was used. A short description of the modeling process is performed below.

On Figures 8-9 there are models which were used in FEA system to control the alignment of the obtained properties to real life ones. In the modeling process only the gauge section of a specimens is used in order to reduce computational complexity.

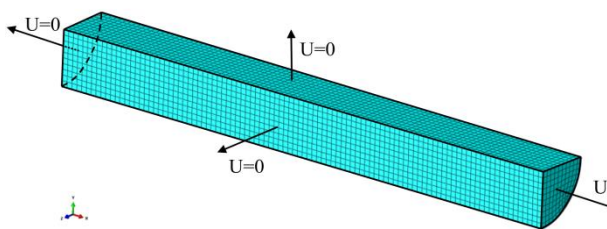


**Figure 8.** Tension model.

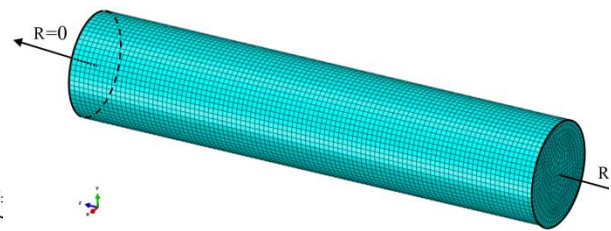


**Figure 9.** Torsion model.

Tension model includes 9600 linear hexa-elements.

Boundary conditions for tension modeling are as follows:

- On the flat side surfaces – symmetry conditions
- On left end surface – zero displacement along normal direction
- On the second opposite end surface – nonzero displacement along normal direction

Torsion model includes 44500 linear hexa-elements.

Boundary conditions for tension modeling are:

- On the one end surface – zero rotation along normal direction
- On the second opposite end surface – nonzero rotation along normal direction

As it seen in above description, we used kinematic boundary conditions. This displacement is applied in 100 steps with linear growth from 0.1% to 100% of its final value. Such way of defining boundary conditions allows to extract stress-strain curve in a resolution good enough to analyze it and compare with experimental data. The displacement is applied to the model through a reference point which is connected with end surface.

## 6. Results

On Fig. 10-13 there is a demonstration of results of finite elements simulation and experimental data. This allows to check the quality of constructed models. Such analysis was performed for each test done. Here there is an example of tests results along Y axis for two proposed materials.

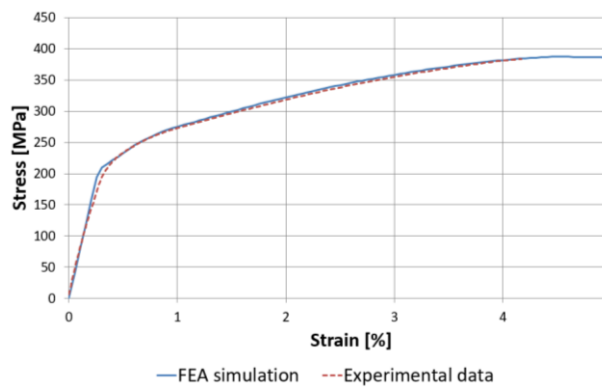


**Figure 10.** Tension model.

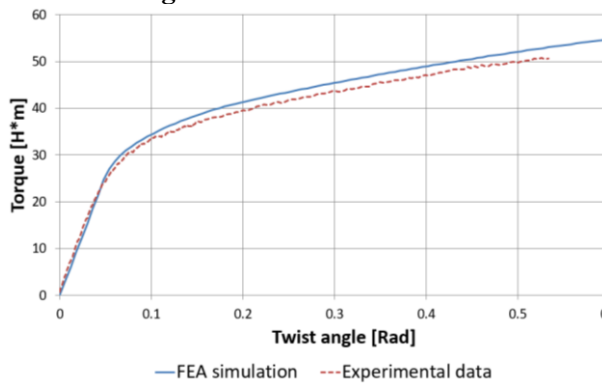


**Figure 11.** Torsion of AlSi10Mg specimen about Y axis.

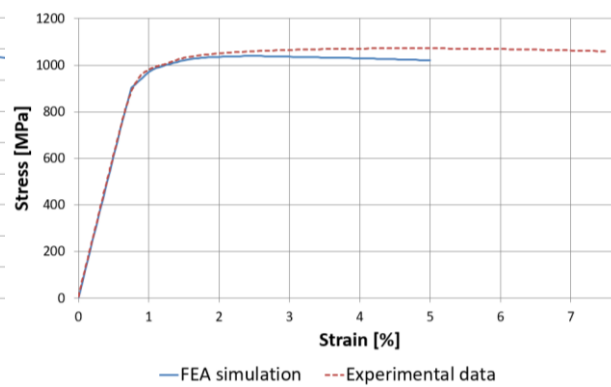


**Figure 12.** Tension model.

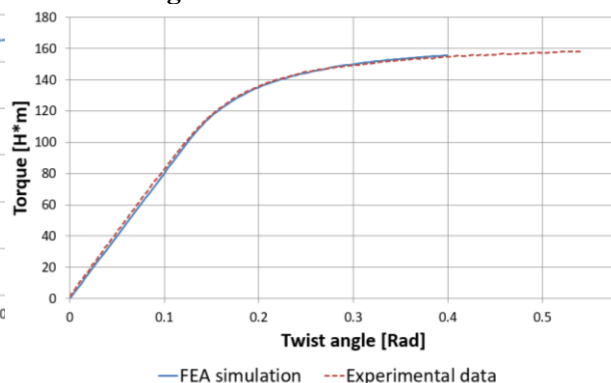


**Figure 13.** Torsion of Ti6Al4V specimen about Y axis.

## 7. Lattice structure FEA simulation

In this part there is an example of using a constructed material model in relatively complicated FEA simulation. This example is needed to demonstrate model applicability to structural analysis. 3d-printed lattice structure was chosen as a design for this research. This choice was made due to the fact that lattice structure is a well-known demonstration of additive manufacturing capabilities in terms of model complicity and further application possibilities.

Performed research was made for aluminum alloy printed lattice and consists of several steps: model preparation, natural testing, FEA simulation, result analysis. Lattices were tested to investigate their behavior in cases of uniaxial tension and compression. We decided to test both tension and compression as the lattice structure behavior may vary depending on the sign of the applied load [15].

### 7.1. Natural testing

As it was mentioned before, uniaxial tension and compression tests were carried out. Since structures have complex geometry, it is not possible to mount them in the test machine directly without any additional gear. So the specimens were adapted to the test machine by adding special blocks for installing. The shapes of the specimens and a basic cell are presented in Fig. 14.

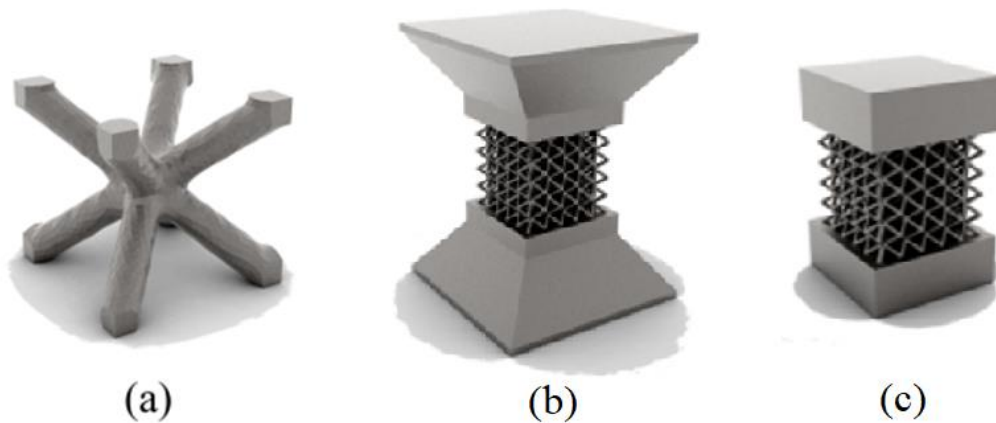


**Figure 14.** Shapes of (a) basic cell of specimen (b) tension specimen (c) compression specimen.

Tests were carried out with Instron 8850 Axial-Torsion System. The photographs of the specimens during tests are shown in Fig. 15.

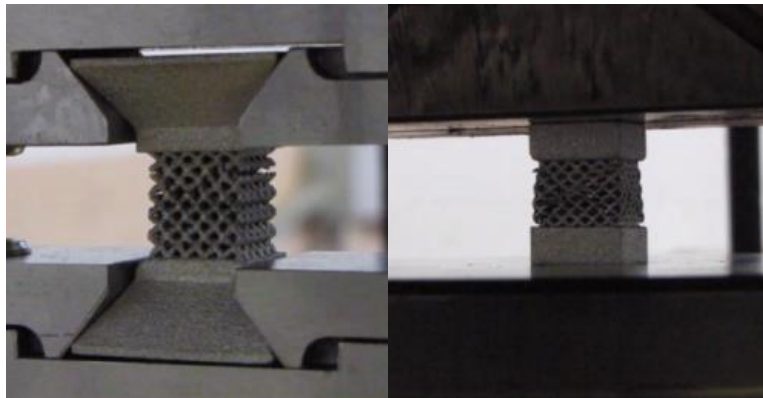


**Figure 15.** Deformed shape of AlSi10Mg specimens.

### 7.2. Finite element modeling

FE modeling of uniaxial tension and compression was performed in SIMULIA Abaqus implicit solver with the same finite element models both for tension and compression. Constructed model is shown in Fig. 16.

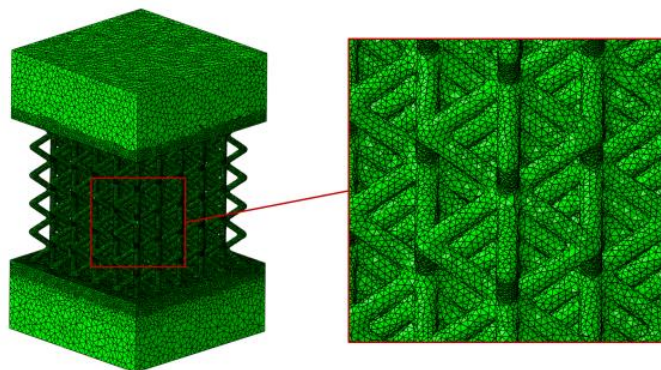


**Figure 16.** Finite element model for modeling of the experiments.

The characteristics of the finite-element model are as follows:

- element type – C3D4 (four-node linear tetrahedra);
- number of elements – 1 156 665;
- number of nodes – 273 733.

During the simulation the bottom face of the specimen is fully fixed, the top face has a prescribed axial displacement.

One run takes about five hours.

### 7.3. Results

On Fig. 17 – Fig. 18 there are curves obtained from the natural testing and FEA modelling. Axes of the curves are: abscissa is the axial reaction force and ordinate is the displacement of the top face.

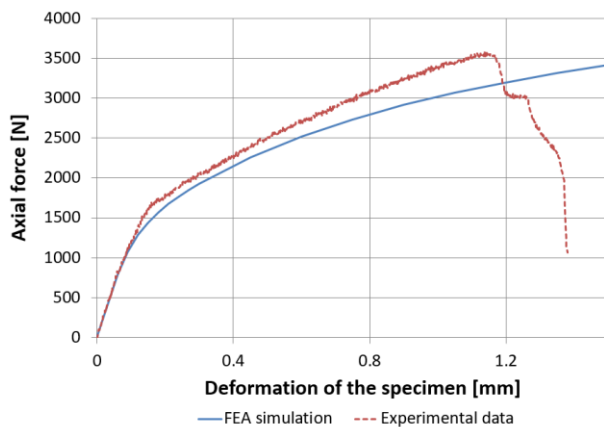


**Figure 17.** Force-deformation curve for tension.

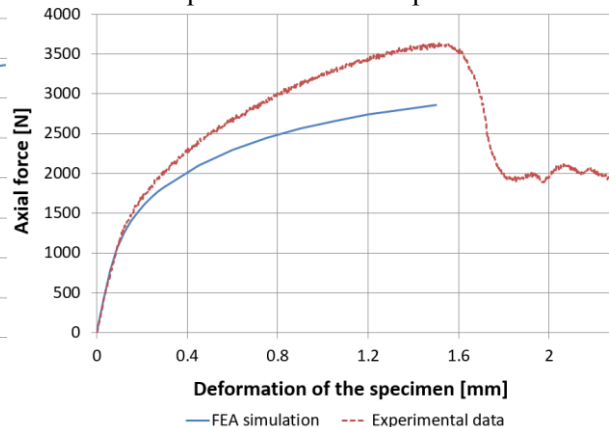


**Figure 18.** Force-deformation curve for compression.

Above figures show that the results of FEA simulation have good correlation in the linear range for both tension and compression cases. Also specimens' behavior at high level of deformation is described by the constructed model quite well. This model doesn't describe fracture region as if we didn't introduce fracture criteria into the model.

## 8. Discussion

In order to prove the assumption of orthotropic material behavior the analysis of material microstructure was performed. The analysis was based on several slice images obtained by using electronic microscopy in different cross-sections. Two of these slices were presented in this paper on Figures 1-2. From the analysis of all these slices several conclusions were made.

Despite the microstructure of researched materials closely matches their cast structure, it was discovered that AlSi10Mg crystallites have pronounced elongation in two orthogonal directions. This can be explained by the influence of the scanning strategy of a printing machine. This means that the path of laser or electron beam may define the shape of crystallites. Such irregularity in crystallite shape causes the differences in material properties in different directions. This can be observed in Table 1. Ti6Al4V structure is relatively more regular than AlSi10Mg one. This also can be observed in the deviations of material properties. Obtained Ti6Al4V constants are closer to each other in comparison to AlSi10Mg ones.

All these conclusions may prove the assumption that additive manufacturing process causes material properties change and that it is the reason of the material anisotropy.

As well there are some conclusions can be made based on the results of finite elements modeling for tested specimens and for lattice structures.

Main conclusion here is that constructed models describe elastic material behavior with high precision both in case of tested specimen and complicated nonlinear structure. This is seen by the coincidence of the linear parts of curves on all the performed the graphs. Moreover, constructed models provide the

moment of transition to plasticity in the right moment in terms of stresses. This is confirmed by curves alignment in the early plasticity section of the graphs. One more point is that the models have noticeable deviations from experiments in the late plasticity region. But the global behavior still described quite well. Such deviations may be caused by the assumption of a single plastic curve which was made before. This assumption gave the possibility to properly and accurate describe transition to the plasticity and its early region, but to describe later regions some more assumptions need to be done.

## 9. Conclusions

All conclusions made before are mostly related to the performed research of material properties of additively produced parts, but not to the proposed methodology of the modeling of these materials which was the main goal of the whole study. Despite all of those conclusions are relevant and may be used in further research, they all are still parts of the methodology, i.e. steps to be done during the material modeling. General conclusions which can be related to the methodology are presented below.

The proposed methodology contains a detailed description of a modeling process of metal materials obtained with layer-by-layer technology. Each step of this modeling process is provided with explanation and theoretical motivation. The example of applying this methodology is made for two additively produced metal alloys (AlSi10Mg and Ti6Al4V).

This methodology allows design and research engineers to easily master the submitted modeling process and know how to build a highly adequate model of additively produced materials for their needs. All the results obtained with the use of this methodology are strongly connected with the manufacturing process (printing machine and settings). This means that it is possible to obtain several different models of one metal material which was produced on different machines. This methodology may be a base for constructing even more complicated models which can contain extra properties for special purposes.

## References

- [1] Jing Zhang and Yeon-Gil Jung Additive 2018 Manufacturing : Materials, Processes, Quantifications and Applications *United Kingdom Butterworth-Heinemann* p 352
- [2] Frazier W E 2014 Metal additive manufacturing: a review *J. Mater. Eng. Perform.* (vol. 23, no. 6) pp 1917–1928
- [3] Polozov I, Sufiiarov V and Popovich A 2020 Investigation of Ti-6Al-4V alloy in situ manufactured using selective laser melting from elemental powder mixture *Solid State Phenomena.* (299:646-651)
- [4] Hiemenz J 2007 Electron Beam Melting *Advanced Materials and Processes* (165(3)) pp 45-46
- [5] Facchini L, Magalini E, Robotti P and Molinari A 2009 Microstructure and mechanical properties of Ti-6Al-4V produced by electron beam melting of pre-alloyed powders *Rapid Prototyp. J.* (15(3)) pp 171–78
- [6] Rosenthal I, Stern A and Frage N 2014 Microstructure and mechanical properties of AlSi10Mg parts produced by the laser beam additive manufacturing (AM) technology *Metallogr. Microstruct. Anal* (3(6)) pp 448– 53
- [7] Carroll BE, Palmer TA and Beese AM 2015 Anisotropic tensile behavior of Ti-6Al-4V components fabricated with directed energy deposition additive manufacturing *Acta Mater.* (87:309–20)
- [8] Popovich A A, Sufiiarov V S, Borisov E V, Polozov I A, Masaylo D V and Grigoriev A V 2017 Anisotropy of mechanical properties of products manufactured using selective laser melting of powdered materials *Russ. J. Non-ferrous Metals* (58) pp 389–395
- [9] Simonelli M, Tse Y Y and Tuck C 2014 Effect of the build orientation on the mechanical properties and fracture modes of SLM Ti–6Al–4V *Mater. Sci. Eng. A* (vol. 616) pp 1–11
- [10] Lehnickii S G 1977 Continuum mechanics of anisotropic body *Moskow. Nauka* p 416
- [11] Pisarenko G S and Mojarovskii N S 1987 Equations and boundary problems of the theory of plasticity and creep: a reference manual (Kiev. Naukova Dumka) p 496.
- [12] USSR Standart 1497-84 Metals 2005 Tension tests methods (Moskow. Standartinform) p 24
- [13] USSR Standart 3565-80 Metals 1980 Torsion tests methods (Moskow. Standarts publishing office) p 17

- [14] Help V 2019 Instron Bluehill 2 Modulus calculations [electronic resource] *Illinois Work Tools, Inc., Norwood* (USA Access mode: <https://www.instron.com>, free)
- [15] Ushijima, Cantwell, Mines, Tsopanos and Smith 2010 An investigation into the compressive properties of stainless steel micro-lattice structures *Journal of Sandwich Structures and Materials* (13) pp 303-29